Accepted Manuscript

Numerical simulations of stratocumulus cloud response to aerosol perturbation

M. Andrejczuk, A. Gadian, A. Blyth

PII: S0169-8095(14)00007-6
DOI: doi: 10.1016/j.atmosres.2014.01.006
Reference: ATMOS 3059

To appear in: *Atmospheric Research*

Received date: 8 March 2013
Revised date: 2 October 2013
Accepted date: 5 January 2014

Please cite this article as: Andrejczuk, M., Gadian, A., Blyth, A., Numerical simulations of stratocumulus cloud response to aerosol perturbation, *Atmospheric Research* (2014), doi: 10.1016/j.atmosres.2014.01.006

Numerical simulations of stratocumulus cloud response to aerosol perturbation

M. Andrejczuk[a], A. Gadian[b], A. Blyth[b]

[a] *Atmospheric, Oceanic and Planetary Physics, Clarendon Laboratory, Parks Road, University of Oxford*
[b] *School of Earth and Environment, University of Leeds*

Abstract

In this paper results from the 2D numerical model with Lagrangian representation of microphysics are used to investigate the response of the radiative properties of stratocumulus as a result of adding aerosol within the boundary layer. Three different cases characterized by low, moderate and high cloud droplet number and for 3 sizes of additional aerosol 0.01 μm, 0.1 μm and 0.5 μm are discussed. The model setup is an idealization of one of the proposed Solar Radiation Management methods to mitigate global warming by increasing albedo of stratocumulus clouds. Analysis of the model results shows that: the albedo may increase directly in response to additional aerosol in the boundary layer; the magnitude of the increase depends on the microphysical properties of the existing cloud, and is larger for cloud characterized by low cloud droplet number; for some cases for clouds characterized by high cloud droplet number seeding may lead to the decrease in albedo when too large radius of seeding aerosol is used.

Keywords: geoengineering; cloud brightening; LES

1. Introduction

Geoengineering of the stratocumulus clouds is proposed as a one of the methods to offset global warming due to a greenhouse gases emission. Various methods are under consideration, aiming to decrease the flux of the solar radiation reaching the Earth surface (Solar Radiation Management, e.g. Shepherd et al. (2009)). One of the proposed methods is cloud brightening (Latham (1990), Latham (2002), Latham et al. (2008) Latham et al. (2012)). In this method reduction of the solar radiation flux is achieved by increasing the cloud albedo - the first indirect effect Twomey (1977), and longevity - the second indirect effect Albrecht (1989), of the low level stratocumulus clouds, by near surface CCN emission.

Climate model simulations (Jones et al. (2009)) indicate that stratocumulus cloud seeding may delay global warming by as much as 25 years, giving the time to adopt or to find a better way to deal with the problem. However the cloud-aerosol interactions and aerosol indirect effect is not fully understood yet, and representation of these processes in climate models are very simplified (e.g. Ghan et al. (2011)). This uncertainty in representation and understanding of the fundamental processes is a source of uncertainty in the climate prediction. In recent years there have been afforts in the scientific community to asses geo-engeneering schemes using climate models (Latham et al. (2012), Korhonen et al. (2010), Jones et al. (2009), Rasch et al. (2009) Latham et al. (2008)), but relatively little research has been devoted to modelling details of these processes and in particular, the single cloud response to additional aerosols emitted into the boundary layer. Limited studies with simpler models than used in this paper, have been conducted in the past to address the effect of the aerosol emission on the cloud in the context of the geo-engineering. Bower et al. (2006) and Latham et al. (2012) assessed validity of cloud modification as a way to offset global warming with parcel model, without taking into account drizzle. This work confirmed an increase of albedo with an increase of cloud droplet number, with the cloud droplet number being the main factor responsible for cloud albedo change. Wang et al. (2011), and Latham et al. (2012) addressed cloud geo-engeenering problem in LES (Large Eddy Simulation) framework, resolving aerosol emission from the surface and transport into the cloud, but with less accurate approach to microphysics, with the similar to Bower et al. (2006) conclusions.

In this study a Lagrangian approach to microphysics (Lagrangian Cloud Model) Andrejczuk et al. (2008), Andrejczuk et al. (2010) is used to investigate the stratocumulus cloud response to aerosol perturbation. Lagrangian approach to microphysics is a new devepment in cloud modelling, aiming to improve representation of microphysics in numerical models. This study does not intend to model all of the details of the aerosol emission from the spray vessels as proposed by (Latham (1990), Latham (2002)), but rather to look at this proproblem in an idealized setup. This paper assumes that emitted aerosol form a well mixed layer below the cloud, with a uniform distribution of aerosol below specified height. Despite this simplification, the process of transport of aerosol from below the cloud into the cloud is represented, and since the boundary layer is typically well mixed there are reasons to believe that aerosol will form such layer with time even when emitted from the surface. We also assume that chemical composition of the aerosol in the boundary layer and that of seeding aerosol is the same ammonium sulphate.

The paper is organized as follows: in section 2 numerical model is described, initial conditions and model setup are described in section 3. Model results are discussed in section 4, and conclusions are in section 5.

2. Numerical model

Numerical model used to simulate cloud response to aerosol perturbation is the Lagrangian Cloud Model (LCM). Detail of the model formulation can be found in Andrejczuk et al. (2010) (coalescence) and Andrejczuk et al. (2008) (condensation/evaporation). The LCM framework represents the dynamics and thermodynamics in a traditional, Eulerian framework, with the details of the Eulerian model described in Reisner et al. (2005), Reisner and Jeffery (2009); whilst the microphysics is represented in Lagrangian framework, with two way coupling between Eulerian and Lagrangian parts. The microphysical (Lagrangian) part traces millions of parcels, each representing milions of aerosol particles having the same chemical composition and physical properties (location, aerosol size, velocity). Depending on the environmental conditions i.e. the solution of the Eulerian part of the model water can condense/evaporate on the surface of these aerosol. Corresponding forces are returned to the Eulerian part to progress model forward in time. Since each Lagrangian parcel represents aerosol having the same physical/chemical properties only one additional parameter to the parcel location, velocity, aerosol and droplet size – number of real aerosol particles Lagrangian parcel represents is required to fully describe properties of the parcel. The model used in this paper is one of three of this type of models recently developed, with other reported by Shima et al. (2009) and Riechelmann et al. (2012).

The coalescence algorithm in the Lagrangian microphysics formulation used in simulations reported in this paper maps the collisions between all Lagrangian parcels within the collision grid on a specified two dimensional Euleran grid (microphysical grid). As a result in coalescence not only droplet sizes are processed but also aerosol sizes, and with time aerosol larger than initially specyfied can form. New parcels are created only for bins, where number of physical particles is greater than a specified number. Combined with the parcel merging algorithm, this makes problem numerically solvable, by keeping the number of parcels relatively low. Both mapping and merging processes conserve mass of the aerosol and mass of the water. Based on sensitivity study discussed in appendix of Andrejczuk et al. (2012), in the simulations reported in this paper collision is called every 1s. Additionally each computatinal grid is split into 4 collision grids.

3. Model set-up and initial conditions

Three 2D idealized cases are considered, with the initial conditions (temperature, qv, horizontal velocity, aerosol distribution) derived from the VOCALS field campaign, Wood et al. (2011). These cases were based on the cloud droplet concentration and for $HIGH$ 250 cm^{-3}, MED - 120 cm^{-3} and for LOW - 65 cm^{-3} were measured. For all three cases, profiles of potential temperature (θ) and water vapour mixing ratio (q_v) were specified as:

$$\theta(z) = \begin{cases} \theta_B, & z \leq z_B; \\ \theta_C + \alpha z, & z_B < z \leq z_T; \\ \theta_T + (z - z_T)^{2.8}, & z > z_T; \end{cases} \tag{1}$$

$$q_v(z) = \begin{cases} q_{vB} \text{ (or saturation)} & \text{if } z \leq z_T; \\ q_{vT} & \text{if } z > z_T; \end{cases} \tag{2}$$

with the constants for each simulation defined in table 1. Initial profiles for the θ and q_v and profiles derived from a model for the last 3 hours for a model output saved every 6 minutes are shown in figure 1. Additionally, in this figure observed profiles of the LWC and droplet concentration are plotted together with a corresponding profiles diagnosed form a model solution.

A 2D assumption means that the flow evolves only in x-y direction; and the variability of the flow in y direction is neglected. Representation of the atmosphere in two dimension is an approximation, but computational expense of this model prohibits the use of three dimensional domain. A comparison of the solutions between two- and three-dimensional models for a convective planetary boundary layer was discussed by Moeng et al. (2004).

The reference runs use two modal log-normal aerosol distribution fitted to the below the cloud Scanning Mobility Particle Sizer (SMPS) observations (table 2), with the coalescence process active starting from 2nd hour. More details about the setup and comparison of the model results with VOCALS observations can be found in Andrejczuk et al. (2012). Sensitivity runs (table 3) were initialized from the reference runs solutions after 4 hours. For the sensitivity runs aerosol of differing concentration and size, were added in the area from 300 meteres below the cloud base to the surface. All sensitivity runs were next run for 6 hours with the coalescence process active. The purpose of the sensitivity runs was to determine response of the cloud to the concentration and size of the additional aerosol. Sensitivity runs are identified by the referrence run for which additional aerosol is added after 4 hours ($HIGH$, MED, LOW), concentration of the additional aerosol added (100, 200, 400, 800 [cm^{-3}]), and size of the additional aerosol (0.1 - p1, 0.5 - p5 [μm]). See table 3 for an overview of all the runs.

For each run, the model output was saved every 10 minutes, and the cloud properties were derived from this output. Three different seeding aerosol sizes were investigated (0.01 μm, 0.1 μm and 0.5 μm), but only simulations using 0.1 μm and 0.5 μm are discussed in details. Seeding with the aerosol size 0.01 μm has little effect on cloud properties, because a negligible fraction of the aerosol with this size grows to sizes bigger than the activation radius. Note that throughout this paper for the cloud droplet we mean a droplet with the size bigger than 1 μm.

4. Results

4.1. Cloud properties

The aim of the 'cloud brightening' approach is to increase albedo of the stratocumulus clouds. For a plane parallel atmosphere and neglecting absorption, cloud albedo can be approximated Meador and Weaver (1980) (see also Twohy et al. (2005)) as a following function of the optical thickness - τ:

$$A = \frac{0.75(1-g)\tau}{1+0.75(1-g)\tau}, \tag{3}$$

where $g = 0.85$ - asymmetry factor. Optical thickness is defined as (e.g. Stephens (1978)):

$$\tau = \int_0^{\Delta z} dz \int_0^{\infty} drQ(x)\pi n(r)r^2, \tag{4}$$

where $Q(x)$ is efficiency factor for extinction, $x = 2\pi r/\lambda$, $n(r)$ - cloud droplet size distribution. For the short-wave radiation variability of $Q(x)$ is small and it approaches asymptotic value of 2. This value was used to calculate optical thickness. Additionally only parcels within the cloud having radius bigger than 1 μm were used for this calculation. For smaller droplet sizes, the efficiency factor for extinction is small and as a result they do not contribute much to the optical thickness.

The left panels of the figure 2 show the evolution in time of the cloud albedo. The solid red colour curve shows the evolution of the albedo for the reference run (without adding aerosol), and solid green/blue/yellow/magenta lines show solutions for perturbation runs with additional aerosol concentrations 100/200/400/800 cm^{-3}, and a dry radius 0.1 μm. Dashed lines show corresponding solutions for the cases when seeding aerosol has a radius 0.5 μm. Each point on the plot represents a space average albedo for the instantaneous solution. The reference runs show that albedo evolution in time is different for each of the cases. It increases with time for the HIGH case, stays approximately constant for the MED and decrease for the LOW. Adding additional aerosol typically increases albedo, with the magnitude of the increase increasing with the increasing concentration of added aerosol. With the few exceptions (MED200p1/MED200p5, HIGH200p1/HIGH200p5, HIGH800p1/HIGH800p5) the effect of seeding aerosol size on albedo change is small - the values of the albedo averaged over the last hour are also shown in table 4.

In figure 2 the grey area shows the standard deviation of the albedo for the referencei run, indicating a significant variation of the albedo within one time-step. For many cases the mean albedo for the perturbation runs is within the variability of the model solution for the reference run. To determine whether the albedo change for the perturbation runs are statistically different from the reference runs, a two sample tests were performed and the results are presented in table 4, together with the mean increase in the albedo for the last hour. Each sample uses the albedo values for the last 1 hour (what gives length of the sample 6*80=480 points). The null hypothesis is that values in perturbation runs are bigger than in corresponding reference run and significance level is specified as 95%. Out of the 24 perturbed runs only 4, for HIGH reference runs, for both seeding aerosol sizes and below the cloud concentrations of 100 and 200 cm^{-3} was rejected. For the remaining 20 perturbation runs increases of the albedo are statistically significant. This increase is different for each of the cases; it is smallest - dA = 1.50 % for the M100p1 and largest - dA=16.80 for the L800p1 run. There is no consistent trend in relation between seeding aerosol size and albedo change and seeding with bigger aerosol sometimes leads to a larger increase in the albedo and sometimes to a smaller increase.

One of the possible side effects of the geo-engineering is that it can effect the cloud in the manner to that intended, that is, it may reduce albedo. For example if the cloud is seeded with too big aerosol. Although we do not find it to be a case for seeding aerosol 0.1 μm, seeding with aerosol 0.5 μm for cases HIGH_100 and HIGH_200 leads to a statistically significant decrease in albedo. This finding is consistent with the results reported by Latham et al. (2012), where decrease of the albedo when seeding with large aerosol was also reported.

The right hand column of figure 2 shows the cloud droplet number concentration (N) for the corresponding albedo plots. The transport of the aerosol is relatively rapid and within the 2 hours from the emission start, the maximum of the cloud droplet number within the cloud is reached for most of the cases. The increase of albedo is accompanied by the increase in the cloud droplet number concentration, indicating that indeed, increase in number leads typically to decrease in droplet size and results in a larger albedo, because of the increase in the droplet surface area as discussed by Twomey (1977). There are, however, cases where, the runs with different aerosol seeding size (e.g. M_800p1/M_800p5 8.5-10h), when for larger cloud droplet number albedo is smaller than for small droplet number. This indicate that for these 2 runs adding aerosol may also modify droplet distribution significantly and/or there is a change in LWP leading to smaller in total droplet surface. For these particulate cases, magenta line in figure 3b and 3e there is a significant increase in droplet concentration for sizes less than 2 μm for the run where the cloud is seeded with aerosol 0.5 μm compared tu run with seeding aerosol size 0.1 μm, and smaller concentration of the 90-100 μm drizzle droplets.

Other spectra in figure 3 show that when cloud droplet number increases, droplet concentration increases also, mainly for the sizes smaller than the size for which distribution has maximum (within the range 1 - 10 μm). Seeding with aerosol of 0.5 μm leads to a much larger concentration of the droplet in the range 1-2 μm than for corresponding run with seeding aerosol size 0.1 μm. For large droplet/drizzle sizes, there is no consistent trend and there are cases where concentration of the drizzle in the perturbed run is bigger than in the reference run, independent on seeding aerosol size.

4.2. Aerosol activation

Since in the microphysical model, full information about aerosol properties within the cloud droplets is kept, aerosol properties within the cloud droplets can be examined. Figure 4 shows the scavenged fraction F_i e.g. Gérémy et al. (2000) for each aerosol bin (the same bin structure as used to map collisions in coalescence algorithm) defined as:

$$Fi = \frac{N_i}{A_i}, \tag{5}$$

where N_i is the number of droplets with radius bigger than 1 μm (these do not have to be bigger than activation radius for given aerosol size) containing aerosol size from the bin i, and A_i is the total number of aerosol particles in the bin i. Only model grids with $q_c > 0.001$ g/kg are taken into account when calculating F_i. The value of 1 indicates that all droplets having aerosol sizes within a given bin have radius bigger than 1 μm, and 0 that none of the aerosol from the bin grew to the size bigger than 1 μm. Figure 4 shows that scavenged fraction is smallest for the small aerosol and approach 100 % for the large aerosol. This is because the small aerosol have small activation radius but require high saturation to grow to a size bigger than activation radius. These, high super-saturations are not found often and as a result the scavenging fraction drops rapidly to 0 for aerosol radius smaller than 0.05 μm. For that reason seeding with the sizes 0.01 μm had almost no effect on the radiative properties of the cloud, almost none of the seeding aerosol had an opportunity to grow to the droplet size.

Figure 4 also shows the different response of the scavenged fraction curves for small 0.1 μm and large 0.5 μm seeding aerosol. Seeding with the large aerosol induces a significant response on the scavenged fraction curves. Curves move to the right indicating that a smaller fraction of the small aerosol grow to the sizes bigger than 1 μm. Since small aerosol activate very quickly it follows that adding large aerosol leads to a decrease in the supersaturation in the seeded clouds compared to the reference solution, due to the faster condensation rate. For a seeding aerosol size 0.1 μm, changes in the scavenged fraction curves are small despite the fact that up to 300 additional droplets grow to a size bigger than 1 μm. Note, however, that the difference in the cloud droplet number between runs with different aerosol seeding size is not very large because for a seeding size 0.5 μm, almost all the seeding aerosol grow to sizes bigger than 1 μm, and for seeding size 0.1 μm around 85 %.

4.3. Bulk properties

With 24 runs in total there is enough data to examine whether more general conclusions can be derived from the results. Figure 5 shows the relationship between the cloud properties and the derived radiative properties of the clouds for all 24 perturbation runs. Changes are calculated with the respect to the corresponding reference run (i.e. without adding aerosol):

$$\Delta X =<< X_p >_x - < X >_x >_t, \tag{6}$$

where X_p is a vector representing values for the perturbation run and X values for reference run, subscript x indicate an averaging in space, over the computation domain; and subscript t indicates an average in time for the last hour of the simulations. Figure 5 shows the relationship between the change of the cloud droplet number and the change in albedo (A), Liquid Water Path (LWP) and effective radius (calculated from relation $r_{eff} = 3/2LWP/\tau$ [Stephens (1978)]), and between the change in LWP and the change in A, together with the last square fit to all data points, and the correlation coefficient. Expectedly, with the increase of the droplet number the albedo is increasing (figure 5a) and the effective radius is decreasing (figure 5b). There is a weak dependence of both dA and dr_{eff} on the seeding aerosol size, being the result of the variability in the cloud droplet spectrum and the droplet number. In addition, figures 5a and 5b show also dependence of the relation between dA/dr_{eff} and dn on a specific case. And for a given change of droplet number simulations with the initial conditions for HIGH group respond with the smaller increase of the albedo (larger decrease of effective radius) than simulations with the initial conditions for the LOW group. Other two right hand plots show a much larger scattering of the data, but an increase of the LWP with the increase of the droplet number, and an increase of albedo with increase of LWP is present. In addition, examination of figure 5b for runs MED_800p1/MED_800p5 shows that there was a decrease in LWP for the MED_800p1 run by about 10 [g/m^2], which also may have contributed to the observed smaller albedo for the run with the larger cloud droplet number.

4.4. Comparison with the ship track observations

Although, there are no direct measurements of cloud response to aerosol emission similar to the setup discussed in this paper, there have been measurements of the cloud properties within the ship tracks. Aerosol emitted by ships sometimes effects clouds in a manner similar to proposed by the geo-engineering approach. At the moment observations in the ship tracks is the only source of data to validate numerical models, so only a qualitatively comparison is possible.

Analysis of 30 ship tracks by Ackerman et al. (2000) showed that LWC (Liquid Water Content) on average decreased slightly within the ship tracks (contrary to results shown in Radke et al. (1989), where a significant increase in LWP within the ship tracks was observed). The observations analysed by Ackerman et al. (2000) showed both an increase and a decrease of LWC within the ship tracks for a single measurement. Results of the simulations discussed in this papre exhibit similar pattern, and averaged over all perturbation runs mean decrease of LWP by $\sim$0.6 g/m^2 is present, with both positive and negative response of LWP to the increase in cloud droplet number (note, however, that in the analysis we used LWP, whereas in observations LWC was used).

Analysis in Ferek et al. (2000), focused mainly on drizzling cases, demonstrated an increase in number concentration and a decrease in the size of cloud droplets within the ship track. Additionally, observations were consistent with the reduction in the drizzle size drops in areas affected by ship emission. The reduction in the drizzle concentration was also observed by Radke et al. (1989), where cloud properties for two ship tracks were analysed. In our simulations, we also observe decrease in the droplet sizes and an increase in concentration for perturbation runs (disregarding the 2 simulations where adding aerosol lead to decrease of cloud droplet number). Especially for the LOW perturbation runs, there is a reduction in maximum drizzle droplet size (but also drizzle concentration) compared to reference run. HIGH and MED perturbation runs also show similar tendency, but there are also cases for these two sets of simulations where either concentration or drizzle droplet sizes or both are larger for the perturbation run than for the reference run.

As far as impact of pollution on droplet number and size is conserned, satelite observations are consistent with those from the aircraft and increase of the cloud droplet number in a ship tracks was reported (Coakley and Walsh (2002), Segrin et al. (2007)). A liquid water path, drizzle rate and albedo of the clouds , however, show dependence not only on aerosol emmited from ships, but also on a cloud regime and vertical structure of the atmosphere (Segrin et al. (2007), Lebsock et al. (2008), Christensen and Stephens (2011), Chen et al. (2012)).

5. Conclusions

The results of the 2D numerical simulations shown in this paper indicate that cloud albedo may increase as a result of the seeding if enough aerosol is delivered into the cloud. For seeding to be efficient the aerosol size must be big enough to grow by condensation to the size, where it can effect the radiative properties of the cloud ($\sim$1 μm) and yet can not be too big to avoid possible problems that may arise when supersaturation field inside the cloud is significantly modified. Based on the scavenged fraction curves, the seeding aerosol size should be bigger than 0.06 μm and smaller than 0.5 μm to most effectively seed clouds (assuming that the seeding aerosol is ammonium-sulphate). Seeding with too large aerosol may also decrease cloud albedo for specific cases, for clouds characterized by high cloud droplet number concentrations (HIGH setup), when concentration of added aerosol is small. However, for these clouds albedo nevertheless increases in time. The results from the sensitivity studies discussed in this paper and observations of the effect of ship emission on stratocumulus clouds discussed by Chen et al. (2012) indicate that cloud response to aerosol emission is more complex than increase of aerosol $\rightarrow$ increase of cloud droplets $\rightarrow$ increase of cloud albedo. Other factors, such as microphysical properties of existing cloud and the vertical structure of the atmosphere may also effect the outcome of the geo-engeneering.

Numerical model results indicate that the transport of aerosol is relatively rapid and the cloud responds with the maximum increase of the albedo within 1–2 hours from the emission for the simulations and the setup discussed in this paper.

Although the model results are consistent with the observations in the ship tracks, dedicated measurements are needed for the quantitative evaluation of the numerical model results.

6. Acknowledgement

This work was supported by NERC grant NE/F018673/1. Observational data was provided by the British Atmospheric Data Centre (BADC). Comments by dr W. Grabowski helped to improve this manuscript.

References

Ackerman, A.S., Toon, O.B., Taylor, J.P., Johnson, D.W., Hobbs, P.V., Ferek, R.J., 2000. Effects of aerosols on cloud albedo: Evaluation of twomeys parameterization of cloud susceptibility using measurements of ship tracks. J. Atmos. Sci. 57, 2684 2695.

Albrecht, B., 1989. Aerosols, cloud microphysics, and fractional cloudiness. Science 245, 12271230.

Andrejczuk, M., Gadian, A., Blyth, A., 2012. Stratocumulus over SouthEast Pacific: Idealized 2D simulations with the Lagrangian Cloud Model. ArXiv e-prints 1211.0193.

Andrejczuk, M., Grabowski, W., Reisner, J., Gadian, A., 2010. Cloud-aerosol interactions for boundary-layer stratocumulus in the lagrangian cloud model. J. Geophys. Res. 115, D22214, doi:10.1029/2010JD014248.

Andrejczuk, M., Reisner, J.M., Henson, B.F., Dubey, M., Jeffery, C.A., 2008. The potential impacts of pollution on a nondrizzling stratus deck: Does aerosol number matter more than type? J. Geophys. Res. 113, D19204, doi:10.1029/2007JD009445.

Bower, K., Choularton, T., Latham, J., Sahraei, J., Salter, S., 2006. Computational assessment of a proposed technique for global warming mitigation via albedo-enhancement of marine stratocumulus clouds. Atmospheric Research 82, 328–336.

Chen, Y., Christensen, M., Xue, L., Sorooshian, A., Stephens, G., Rasmussen, R., Seinfeld, J., 2012. Occurrence of lower cloud albedo in ship tracks. Atmos. Chem. Phys. 12, 8223–8235.

Christensen, M.W., Stephens, G.L., 2011. Microphysical and macrophysical responses of marine stratocumulus polluted by underlyng ships: Evidence of cloud deepening. J. Geophys. Res. 116, D03201,doi:10.1029/2010JD014638.

Coakley, J.A., Walsh, C.D., 2002. Limits to the aerosol indirect radiative effect derived from observations of ship tracks. J. Atmos. Sci. 59, 668680.

Ferek, R., Garrett, T., Hobbs, P., Strader, S., Johnson, D., Taylor, J., Nielsen, K., Ackerman, A., Kogan, Y., Liu, Q., Albrecht, B., Babb, D., 2000. Drizzle suppression in ship tracks. J. Atmos. Sci. 57, 2707–2728.

Gérémy, G., Wobrock, W., Flossmann, A., Schwarzenbock, A., Mertes, S., 2000. A modelling study on the activation of small aitken-mode aerosol particles during cime 97. Tellus B 528, 959979.

Ghan, S.J., Abdul-Razzak, H., Nenes, A., Ming, Y., Liu, X., Ovchinnikov, M., Shipway, B., Meskhidze, N., Xu, J., Shi, X., 2011. Droplet nucleation: Physically-based parameterizations and comparative evaluation. J. Adv. Model. Earth Syst. 3, M10001, doi:10.1029/2011MS000074.

Jones, A., Hayward, J., Boucher, O., 2009. Climate impacts of geoengineering marine stratocumulus clouds. J. Geophys. Res. 114, D10106.

Korhonen, H., Carslaw, K.S., Romakkaniemi, S., 2010. Enhancement of marine cloud albedo via controlled sea spray injections: a global model study of the influence of emission rates, microphysics and transport. Atmos. Chem. Phys. 10, 4133–4143.

Latham, J., 1990. Control of global warming? Nature 347, 339340.

Latham, J., 2002. Amelioration of global warming by controlled enhancement of the albedo and longevity of low-level maritime clouds. Atmos. Sci. Lett. , doi:10.1006/asle.2002.0048.

Latham, J., Bower, K., Choularton, T., Coe, H., Connolly, P., Cooper, G., Craft, T., Foster, J., Gadian, A., Galbraith, L., Iacovides, H., Johnston, D., Launder, B., Leslie, B., Meyer, J., Neukermans, A., Ormond, B., Parkes, B., Rasch, P., Rush, J., Salter, S., Stevenson, T., Wang, H., Wang, Q., Wood, R., 2012. Marine cloud brightening. Phil. Trans. Roy. Soc. A 370, 42174262.

Latham, J., Rasch, P., Chen, C.C., Kettles, L., Gadian, A., Gettelman, A., Morrison, H., Bower, K., Choularton, T., 2008. Global temperature stabilization via controlled albedo enhancement of low-level maritime clouds. Phil. Trans. Roy. Soc. A 366, 39693987.

Lebsock, M.D., Stephens, G.L., Kummerow, C., 2008. Multisensor satellite observations of aerosol effects on warm clouds. J. Geophys. Res. 113, D15205, doi:10.1029/2008JD009876.

Meador, W., Weaver, W.R., 1980. Two-stream approximations to radiative transfer in planetary atmospheres: A unified description of existing methods and a new improvement. J. Atmos. Sci. 37, 630643.

Moeng, C., McWilliams, J.C., Rotunno, R., Sullivan, P.P., Weil, J., 2004. Investigating 2d modeling of atmospheric convection in the pbl. J. Atmos. Sci. 61, 889903.

Radke, L.F., J. A. Coakley, J., King, M.D., 1989. Direct and remote sensing observations of the effects of ships on clouds. Science 246, 1146–1149.

Rasch, P., Latham, J., Chen, C.C., 2009. Geoengineering by cloud seeding: influence on sea ice and climate system. Environ. Res. Lett. 4, 045112.

Reisner, J.M., Jeffery, C., 2009. A smooth cloud model. Mon. Wea. Rev. 137, 18251843.

Reisner, J.M., Mousseau, V., Wyszogrodzki, A., Knoll, D., 2005. A fully implicit hurricane model with physics-based preconditioning. Mon. Wea. Rev. 133, 1003–1022.

Riechelmann, T., Noh, Y., Raasch, S., 2012. A new method for large-eddy simulations of clouds with lagrangian droplets including the effects of turbulent collision. New J. Phys. 14, 10.1088/1367–2630/14/6/065008.

Segrin, M.S., Coakley, J., Tahnk, W.R., 2007. Modis observations of ship tracks in summertime stratus off the west coast of the united states. J. Atmos. Sci. 64, 43304345.

Shepherd, J., et al., 2009. Geoengineering the Climate: Science, Governance and Uncertainty. Technical Report 10/09 RS1636. Royal Society.

Shima, S., Kusano, K., Kawano, A., Sugiyama, T., Kawahara, S., 2009. The super-droplet method for the numerical simulation of clouds and precipitation: a particle-based and probabilistic microphysics model coupled with a non-hydrostatic model. Quart. J. Roy. Meteor. Soc. 135, 1307–1320.

Stephens, G.L., 1978. Radiation profiles in extended water clouds. II: Parameterization schemes. J. Atmos. Sci. 35, 2123–2132.

Twohy, C.H., Petters, M.D., Snider, J.R., Stevens, B., Tahnk, W., Wetzel, M., Russell, L., Burnet, F., 2005. Evaluation of the aerosol indirect effect in marine stratocumulus clouds: Droplet number, size, liquid water path, and radiative impact. Journal of Geophysical Research: Atmospheres 110.

Twomey, S., 1977. The influence of pollution on the shortwave albedo of clouds. J. Atmos. Sci. 34, 1149–1152.

Wang, H., Rasch, P., Feingold, G., 2011. Manipulating marine stratocumulus cloud amount and albedo: a process-modelling study of aerosol-cloud-precipitation interactions in response to injection of cloud condensation nuclei. Atmos. Chem. Phys. 11, 42374239.

Wood, R., Mechoso, C.R., Bretherton, C.S., coauthors, 2011. The vamos ocean-cloud-atmosphere-land study regional experiment (VOCALS-REx): Goals, platforms and field operations. Atmos. Chem. Phys. Discuss. 11, 627–654.

Table 1: Constants used to define profiles of the potential temperature, water vapour mixing ratio and cloud water mixing ratio.

RUN	z_B [m]	z_T [m]	θ_B [K]	θ_C [K]	θ_T [K]	q_{vB} [g/kg]	q_{vT} [g/kg]	α [K/m]
HIGH	800	1380	291.1	293.0	302.5	8.3	0.3	3.3×10^{-3}
MED	1000	1400	289.2	290.4	299.0	7.0	0.7	3.0×10^{-3}
LOW	900	1260	290.1	291.1	301.0	7.8	0.7	2.8×10^{-3}

Table 2: Parameters of log-normal distributions used in simulations.

RUN	$N_1[cm^{-3}]$	$r_1[\mu m]$	σ_1	$N_2[cm^{-3}]$	$r_2[\mu m]$	σ_2
HIGH	380	0.071	0.45	160	0.029	0.31
MED	118	0.10	0.43	129	0.022	0.36
LOW	42	0.11	0.25	111	0.023	0.47

Table 3: Overview of the runs. N_a is an aerosol concentration added for each grid from 300 meters bellow cloud base to surface, r_a - radius of the additional aerosol.

RUN	r_a μm	$N_a[cm^{-3}]$
HIGH	-	-
HIGH100p1	0.1	100
HIGH200p1	0.1	200
HIGH400p1	0.1	400
HIGH800p1	0.1	800
HIGH100p5	0.5	100
HIGH200p5	0.5	200
HIGH400p5	0.5	400
HIGH800p5	0.5	800
MED	-	-
MED100p1	0.1	100
MED200p1	0.1	200
MED400p1	0.1	400
MED800p1	0.1	800
MED100p5	0.5	100
MED200p5	0.5	200
MED400p5	0.5	400
MED800p5	0.5	800
LOW	-	-
LOW100p1	0.1	100
LOW200p1	0.1	200
LOW400p1	0.1	400
LOW800p1	0.1	800
LOW100p5	0.5	100
LOW200p5	0.5	200
LOW400p5	0.5	400
LOW800p5	0.5	800

Table 4: Results of the statistical testing of the null hypothesis that albedo for perturbation run is bigger than for reference run with 5% significance level. Y - hypothesis is true, N - hypothesis is false, $*$ indicates that hypothesis that albedo for reference run is bigger than for perturbation run is true. Additionally averaged over the last hour change in the albedo Δ_A=A_p-A_r for each perturbation run is also shown.

RUN	$A_p > A_r$	Δ_A (1 hour mean)	Δ_A (1 hour mean)	$A_p > A_r$	RUN
HIGH100p1	N	0.4	-2.5	N*	HIGH100p5
HIGH200p1	N	0.1	-2.0	N*	HIGH200p5
HIGH400p1	Y	2.3	1.1	Y	HIGH400p5
HIGH800p1	Y	3.9	3.6	Y	HIGH800p5
MED100p1	Y	1.5	2.1	Y	MED100p5
MED200p1	Y	4.9	3.0	Y	MED200p5
MED400p1	Y	5.4	4.5	Y	MED400p5
MED800p1	Y	7.8	9.0	Y	MED800p5
LOW100p1	Y	6.0	6.6	Y	LOW100p5
LOW200p1	Y	10.4	9.0	Y	LOW200p5
LOW400p1	Y	11.7	12.4	Y	LOW400p5
LOW800p1	Y	16.8	17.5	Y	LOW800p5

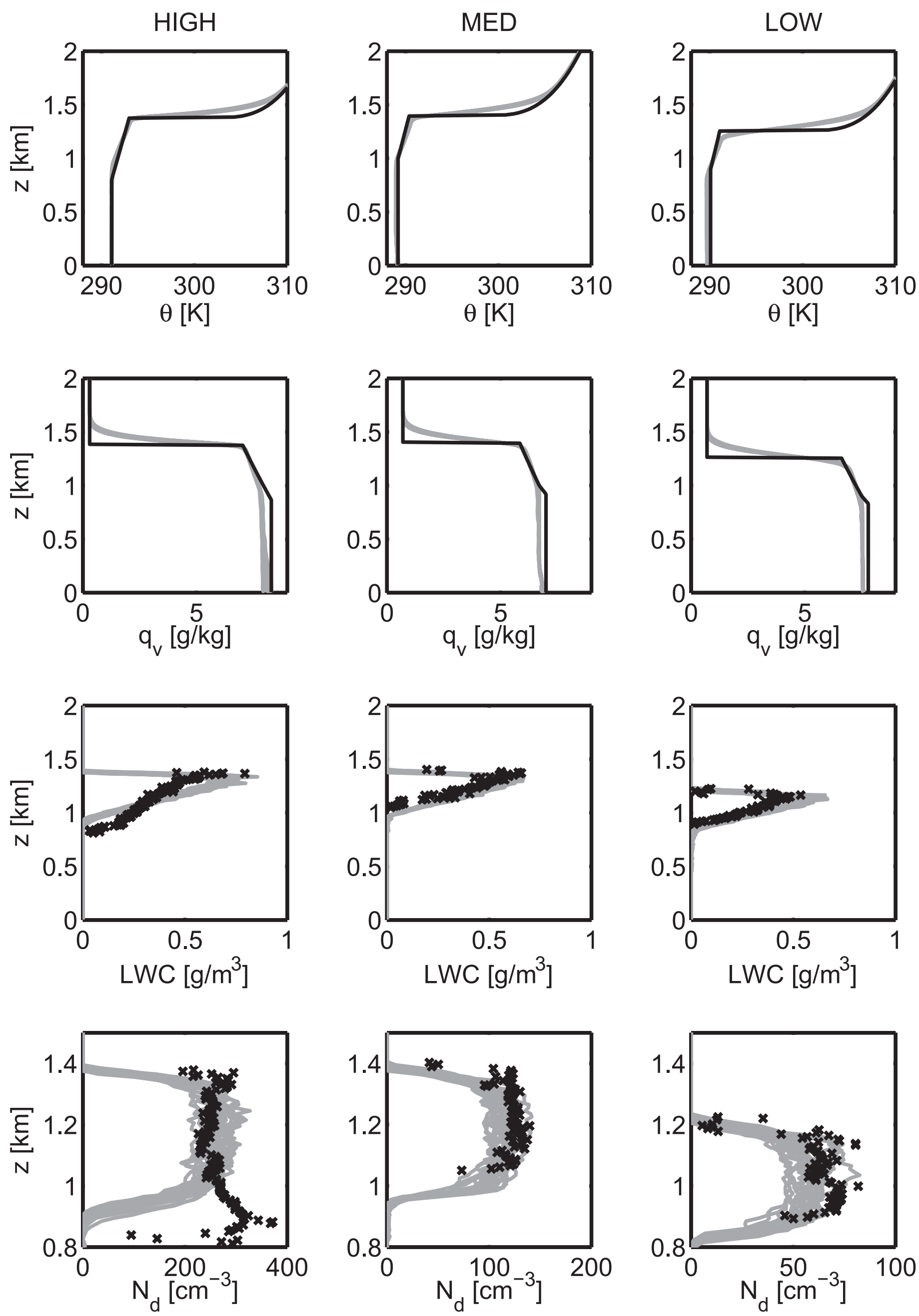

Figure 1: Initial profiles (solid black lines)/observations (black symbols) of potential temperature (θ), water vapour mixing ratio (q_v), Liquid Water Content (LWC), and cloud droplet number(N_d); and model solution for the last 3 hours for a reference setups (gray lines) - HIGH (left column), MED (middle column) and LOW (right column).

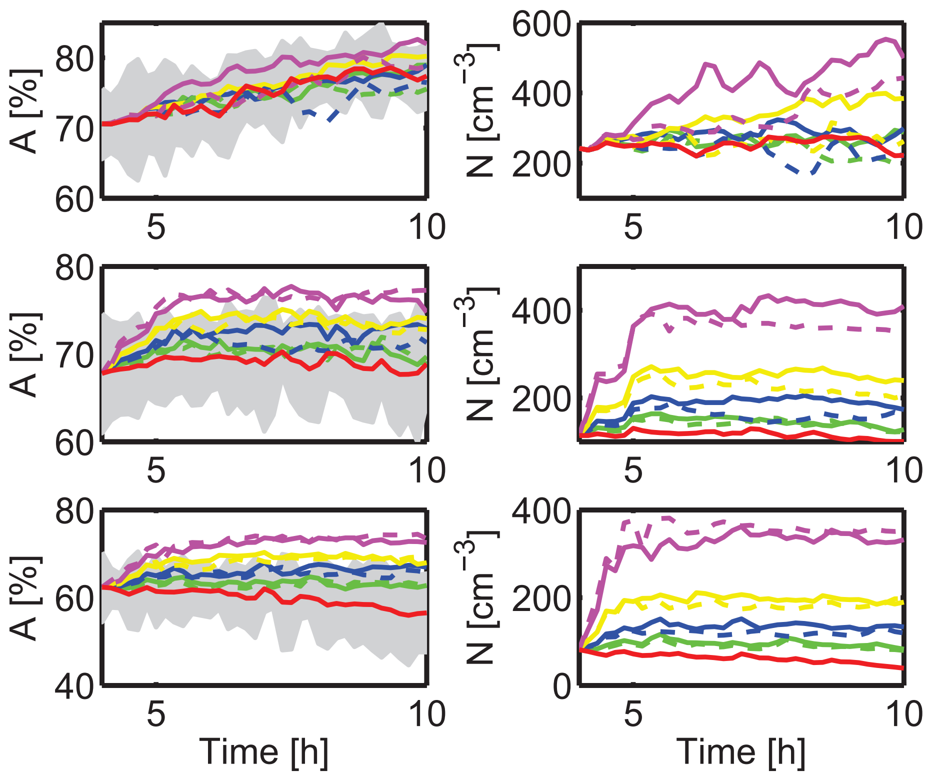

Figure 2: Evolution in time of cloud albedo (left column) and cloud droplet concentration (right panel) for HIGH (a and b), MED (c and d) and LOW (e and f) aerosol distribution. Colors mark different sensitivity simulation: red - reference simulation, green - run with additional aerosol concentration 100, blue - with additional concentration 200, yellow - with additional concentration 400, and magenta - with additional concentration 800 [cm^3] . Solid line - perturbing aerosol size 0.1 μm, dashed line - perturbing aerosol size 0.5 μm

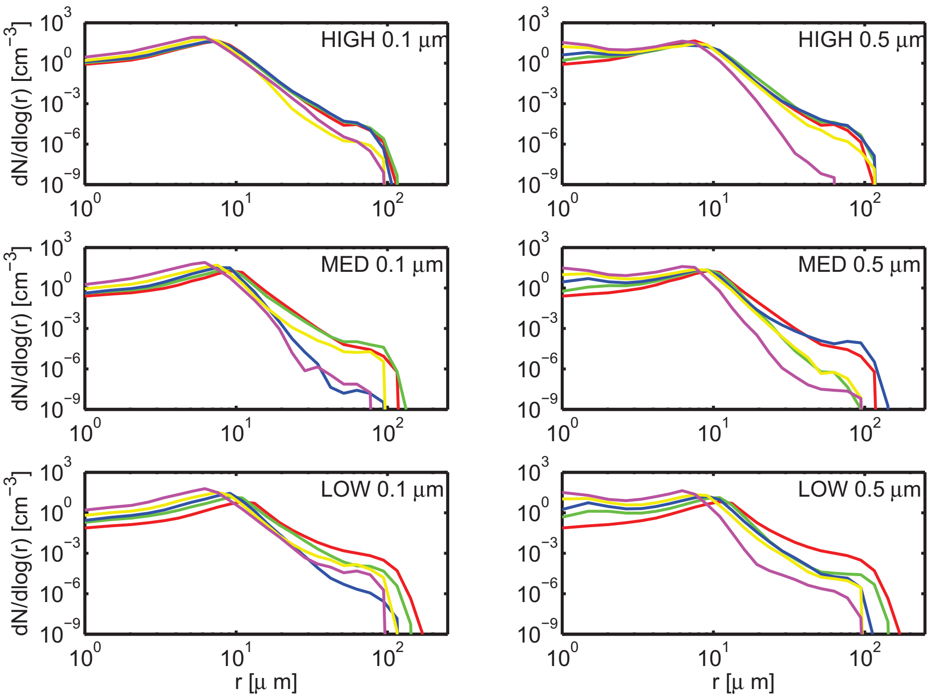

Figure 3: Averaged over the last hour of simulation cloud droplet spectra for perturbing aerosol 0.1 μm (left column) and 0.5 μm (right column).Colors the same as in Fig. 1.

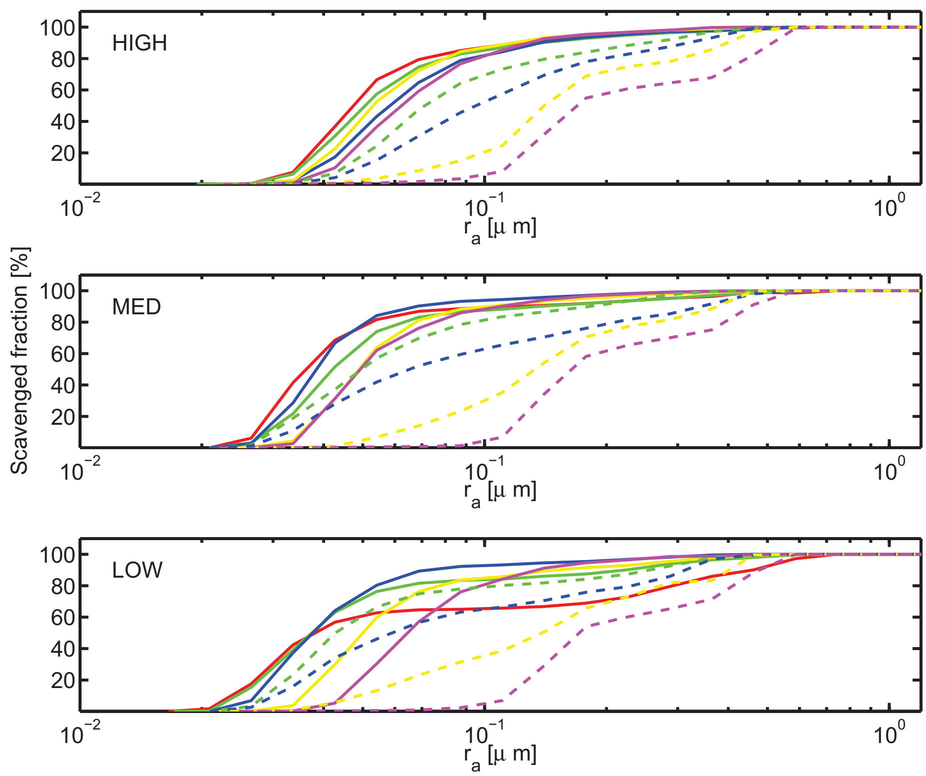

Figure 4: Scavenging fraction averaged over the last hour. Solid line for perturbing aerosol size 0.1 μm, dashed line - perturbing aerosol size 0.5 μm. Colours as in Fig 1.

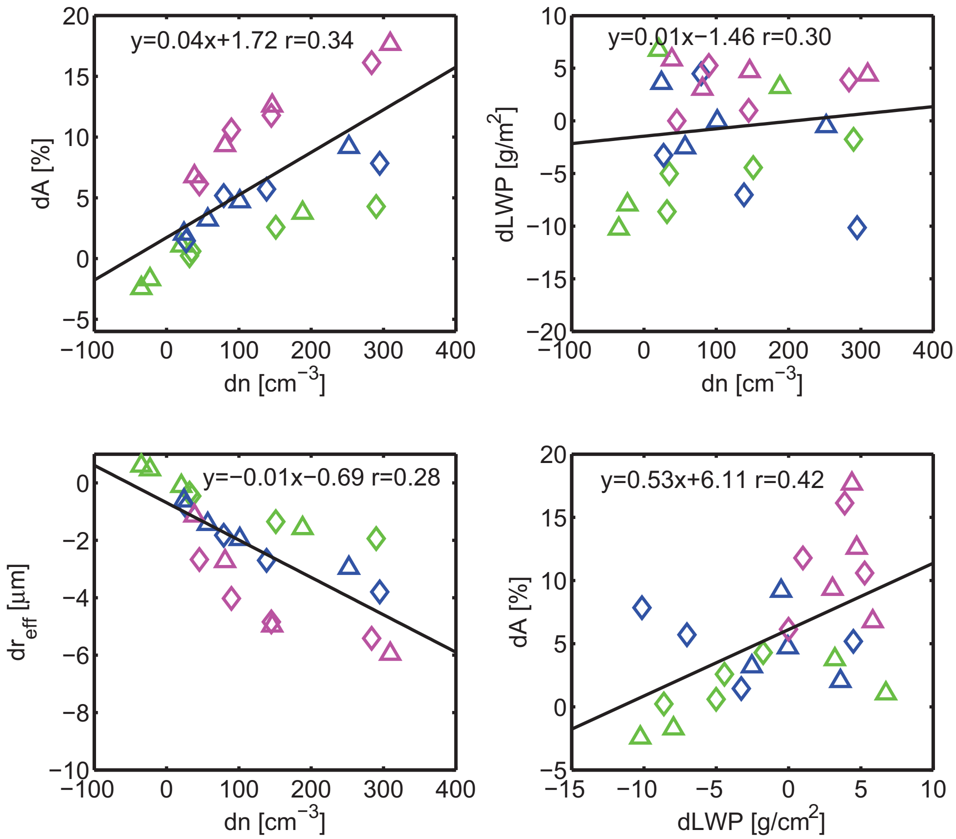

Figure 5: Relation between dn and dA - panel a, dn and $dLWP$ - panel b, dn and dr_{eff} - panel c and $dLWP$ and dA - panel d. Green symbols - perturbation runs with HIGH initial conditions, blue - perturbation runs with MED initial conditions, magenta symbols - perturbation runs with LOW initial conditions. Triangles - perturbing aerosol size 0.5 μm, diamonds - perturbing aerosol size 0.1 μm. Black lines - least square fit to all data points. Additionally each figure contains values of the fit and corellation coefficient for each relation.

Highlights:
Numerical simulations aiming to investigate one of the proposed Solar Radiation Management methods in an idealized setup show that:
1) the albedo may increase directly in response to additional aerosol in the boundary layer,
2) the magnitude of the increase depends on the microphysical properties of the existing cloud, and is larger for cloud characterized by low cloud droplet number,
3) for some cases, for clouds characterized by high cloud droplet number, seeding may lead to the decrease in albedo when too large radius of seeding aerosol is used.